



Risedronate transdermal delivery system based on a fumaric copolymer for therapy of osteoporosis



Magalí Pasqualone^a, Héctor A. Andreetta^b, M. Susana Cortizo^{a,*}

^a Instituto de Investigaciones Físicoquímicas Teóricas y Aplicadas (INIFTA), CONICET, CCT-LaPlata, La Plata, Argentina

^b Laboratorio de Farmacotécnica, Departamento Ciencias Biológicas, Facultad de Ciencias Exactas, Universidad Nacional de La Plata (1900), La Plata, Argentina

ARTICLE INFO

Article history:

Received 27 December 2016

Received in revised form 8 March 2017

Accepted 13 March 2017

Available online 18 March 2017

Keywords:

Fumaric copolymer

Bisphosphonate

Transdermal drug delivery system

Kinetic release

ABSTRACT

Transdermal drug delivery system (TDDS) could be seen as alternative to the oral administration which avoids several adverse effects. In this study a novel TDDS for risedronate (RI), a bisphosphonate used for osteoporosis treatment, based on a vinyl acetate-dioctylfumarate copolymer, poly(VA-co-DOF), previously synthesized, was developed. Two membranes including 6 and 12% (w/w) of drug were obtained, which exhibited good transparency and homogeneous drug distribution, as evaluated by optical microscopy. FTIR spectroscopy and differential scanning calorimetry (DSC) analysis showed no significant drug/polymer interactions, only a plasticizer effect. A new reverse phase high-performance liquid chromatography (RP-HPLC) method for quantification of RI was developed and validated, which demonstrate good linearity, reproducibility and accuracy with limits of detection (LOD) and quantification (LOQ) of 0.38 µg/mL and 1.17 µg/mL, respectively. High drug load efficiency and great drug stability were found. The analysis of the drug release kinetics, fitting to Ritger-Peppas model, leads to values of the diffusion coefficient (n) of 1.37 and 1.05, for 6 and 12% (w/w) RI, respectively. These results correspond to super case transport II and suggest a complex transport mechanism, regulated by the mobility of the polymer chains. Together, these results indicate that this new TDDS could be useful for osteoporosis treatment without adverse effect.

© 2017 Elsevier B.V. All rights reserved.

1. Introduction

Nowadays, the loss of bone mass associated to aging or in postmenopausal women is considered as a major health issue in the world population [1]. This problem is a prerequisite for the occurrence of osteoporosis, which is responsible for the increasing number of fractures observed in adulthood. In search of a preventive treatment for reduce the loss of bone mass, replacement therapies with hormone or the use of various drugs; including bisphosphonates have been applied [2–5]. Bisphosphonates are synthetic compounds structurally related to pyrophosphate, including a P–C–P bridge in their structure, and are inhibitors of bone resorption mediated by osteoclasts [6]. Besides of its application in the treatment of osteoporosis, bisphosphonates have been used in various bone diseases such as Paget's disease and bone metastasis [7, 8]. In particular, it has been shown that risedronate is a potent inhibitor of farnesyl pyrophosphate synthase on *Trypanosoma cruzi*, the agent responsible for Chagas' disease [9].

The pharmaceutical formulation traditionally used for administration of bisphosphonates is the oral dosage form, which has been

associated with adverse events from the upper gastrointestinal tract, acute phase response, hypocalcaemia and secondary hyperparathyroidism, musculoskeletal pain, osteonecrosis of the jaw and ocular events [10]. These drawbacks are related to the high precipitability of bisphosphonates against divalent ions in the circulating blood plasma, which can be recognized by the reticuloendothelial system as a foreign substance [11]. It is known that an alternative to oral route used for drug administration that reduce the gastrointestinal problems, are the transdermal drug delivery systems (TDDS) which are based on different kind of membranes [12]. The correct design of such membranes enables a strict control of different factors such as the site and area of application, amount of drug loaded, absorption speed and ease of self-administration. Thus, the gradual release of active ingredient from the transdermal system allows achieving more stable plasma levels versus time with less variability regarding the routes of oral administration.

Although the administration of bisphosphonates through TDDS appear potentially attractive, in order to overcome the before mentioned problems derived from the oral route, very few of them have been successful performed; mainly due to their high hydrophilicity which limited the transport through the lipid layers of the stratum corneum [1]. Commercial acrylic copolymers were used to design an alendronate transdermal delivery system and the effect of the inclusion of different

* Corresponding author.

E-mail address: gcortizo@inifta.unlp.edu.ar (M.S. Cortizo).

fatty acids on the drug permeation through excised hairless mouse skin was evaluated [13]. Other transdermal delivery system of alendronate was developed using a hydrophilic patch which effectively suppressed the decrease in bone mass in model rats with osteoporosis [14]. Nam et al. [15], proposed the risedronate ion-pair formation in order to enhance the penetration of the bisphosphonate across the skin of hairless mouse. Under the studied conditions, the ion-paired risedronate proved to be 36 times more effective than risedronate alone and thus would be appropriate for a TDDS.

We previously designed a poly(VA-co-DOF)-based membrane, which were transparent, with good mechanical properties and exhibited a non-Fickian water transport mechanism, indicating that the release of a drug will be governed by the relaxation of the polymer chains [16]. As a continuation of our work, we present the results of the characterization of a novel risedronate transdermal delivery system and the drug release kinetic study. We selected risedronate because is known that this bisphosphonate exhibited higher antiresorptive potency than alendronate [17].

2. Experimental

2.1. Materials

3-pyridylacetonitrile (98%, density, 1.108 g/mL), methanesulfonic acid ($\geq 99.5\%$, density, 1.481 g/mL), phosphorus trichloride (99%, density, 1.574 g/mL), tetrabutyl-ammonium bromide (TBAB) were purchased from Sigma-Aldrich (Buenos Aires, Argentina). Polyvinyl alcohol (PVA, $M_w = 72,000$ g/mol, hydrolysis degree $>98\%$), vinyl acetate (VA, 99%), isopropyl alcohol and benzoyl peroxide (PB, recrystallized from methanol) were purchased from Merck (Buenos Aires, Argentina).

2.2. Synthesis of copolymer and risedronate

Copolymer of vinyl acetate and dioctylfumarate, poly(VA-co-DOF) was synthesized by radical copolymerization under microwave conditions as was previously published [16]. The copolymer used in this study, was obtained with 28% conversion of soluble fraction (gel fraction no determined) and a composition of 63:37 (VA:DOF) as evaluated by ^1H NMR spectroscopy. Weight average molecular weight (M_w) and polydispersity index (PI) of 419 kDa and 5.5 respectively. The high polydispersity index found in the molecular weight distribution of poly(VA-co-DOF), indicated that the chain transfer reaction was the predominant chain termination mechanism. During this process a non-crosslinked branched polymers fraction, but soluble, is formed by transfer reaction from the growing macroradical to polymer, while the gel fraction correspond to crosslinked structures. This mechanism involves abstraction of hydrogen atoms via H-abstraction from both backbone tertiary C—H bonds and alkyl side groups, as was previously demonstrated [16].

Risedronate [2-(3-pyridyl)-1-hydroxy-ethane-1,1-bisphosphonate, monosodium salt] was synthesized by an adaptation of a methodology previously described [18]. Briefly, an aqueous methanesulfonic acid solution (85%, 7.06 mL, 8.89 g, 92.5 mmol) was added to 3-pyridylacetonitrile (1.48 mL, 1.64 g, 13.9 mmol) and heated to 98–100 °C for 8 h with mechanical agitation. Then, the reaction temperature was cooled at 65 °C and phosphorous trichloride (4.11 mL, 6.47 g, 47.0 mmol) was added over 25 min. After 5 h. stirring at 65–70 °C, the reaction mass temperature was cooled to 30 °C and pre-cooled water (16.34 mL) was very slowly added in 30 min. The reaction mixture temperature was heated to 98 °C, after 15 h mechanical stirring, the temperature was cooled to 50 °C and the pH was adjusted to 4.3 with NaOH (30% w/v). Finally, methanol (24.5 mL) was added in order to isolate the drug. After 2 h stirring at 5–10 °C, the product was collected by filtration and dried to constant weight. Fig. 1 shows the structure of the obtained product. Yield, 83%; white crystalline solid; Mp: 220 °C. The identification was made by spectroscopic methods.

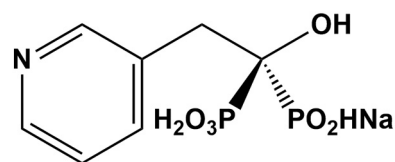


Fig. 1. Structure of synthesized risedronate.

2.3. Techniques of characterization

^1H NMR and ^{13}C NMR spectra of risedronate were recorded with aVariam-200 MHz (Mercury 200) at 35 °C in D_2O . Tetramethylsilane (TMS) was used as an internal standard.

Fourier transform infrared spectra (FTIR) of the polymer films deposited onto a sodium chloride (NaCl) window, stating of a chloroform solution (10% (w/v)) were recorded on a Nicolet 380 FTIR (Thermo Electron Corporation, Madison WI, USA) between 4000–400 cm^{-1} with a resolution of 4 cm^{-1} and 32 accumulated scans. The EZ-OMNIC software (EZOMNIC 7.4.127, Thermo Fisher Scientific Inc., Madison, WI, USA) was used to analyze the spectra. The FTIR of risedronate was obtained from KBr tablets.

Fourier transform infrared spectra (FTIR) (ν , cm^{-1}): 3568, 3360 (OH, free and associated), 1635, 1568 and 1478 (C—C, C—N heterocyclic), 1319 (P=O), 1080, 1048 and 1007 (PO_3), 800 (C—H, out-of-plane, pyridine), 627 (OH out-of-plane bend). ^1H NMR (D_2O): δ (ppm), 3.43 (t, 2H), 7.89, (m, 1H), 8.50(d, 2H), 8.70(s,1H). ^{13}C NMR (D_2O): δ (ppm), 36.4, 73.9, 126.2, 138.3, 138.8, 142.6, 143.3.

Glass transition temperatures (T_g) were measured using a differential scanning calorimeter (Shimadzu-TA60). Samples (~5 mg) were weighed and scanned at 10 °C/min from –50 to 175 °C under dry nitrogen (30 mL/min). Three consecutive scans were performed for each sample: heating/cooling/heating.

2.4. Drug/copolymer interaction study

In order to search possible interaction between RI and polymeric material of the membranes, FTIR and DSC analysis were carried out on pure substances (fumaric copolymer) and their physical mixtures.

2.5. TDDS preparation and drug load efficiency

The membranes with and without risedronate (RI) were prepared following the procedure previously published [16]. Two different amounts (6 or 12% (w/w), in ratio of polymer content) of RI were added to the polymer solution (in ethyl acetate). The dispersions were sonicated using Bandelin Sonorex RK100 equipment, during 15 min and then processed as previously indicated. The thickness of the membrane was measurement at several points using a micrometer and the mean values were calculated.

The drug load efficiency was evaluated through the HPLC analysis of the remaining drug mass in the container of preparation of solutions, after casting. This analysis was carried out by triplicated for the two evaluated concentrations.

2.6. Morphological characterization of TDDS

The thicknesses of the membranes were measured using a Mauer micrometer. The appearance of the membranes were evaluated by direct observation, in order to analyze the homogeneity of drug dispersion, as well as by light microscopy using an Olympus BX51 (Olympus Corp., Tokyo, Japan) connected to an Olympus DP71 (Olympus Corp., Tokyo, Japan) color video camera.

2.7. Drug solution stability

The stability of RI was studied by controlling the RI tittle of two standard solutions (low and high concentration) in phosphate buffer (pH = 7.5), which were maintained at 34.0 °C in culture oven (SAN JOR, Model SL20CDB, accuracy ± 0.1 °C) for 9 consecutive days. The title of the patterns was evaluated daily by HPLC, as well as UV–Vis spectra, in order to observe the existence of any variation in the absorption bands. The analysis was performed in triplicate.

2.8. HPLC analysis of risedronate

Risedronate concentration was analyzed using ion-pair reverse-phase high-performance liquid chromatography (RP-HPLC) method developed in this work and based on adaptation of a previously reported methodology [19]. Hewlett Packard HP 1100, HPLC equipment with UV detection was used. Diode array detector was set at 262 nm (wavelength of maximum absorption of RI, previously determined). Chromatographic separations and subsequent quantifications were carried out at room temperature using a ZOBAX Eclipse XDB-C18 (4.6 \times 150 mm, 5 μ m) reverse phase column. The mobile phase for separation of RI consisted of buffer (5 mM TBAB, 2.5 mM KH₂PO₄, 8.5 mM Na₂HPO₄, pH 7.45) – methanol (75:25 (v/v)), and was pumped at a flow rate of 1.0 mL/min at 25 °C. Mobile phase was filtered before use (Nylon membranes, 0.45 μ m, 13 mm, Osmonics Inc.). The injection volume was 100 μ L and each sample was analyzed by triplicated. Peak areas were used for quantitative analyses. Calibration curve of peak areas versus RI concentration was made by different dilution of a stock solution (0.1 mg/mL), which was linear between 4.3 and 87.1 μ g/mL.

2.9. Validation of the HPLC methodology

The validation of analytical HPLC method was carried out by determining the following parameters: linearity, repeatability, accuracy, limits of quantification and detection (LQ and LD, respectively) [20].

The linearity was performed with a five-point calibration curve and was analyzed in duplicated. The slope and the intercept of the calibration graph were calculated by linear regression of the risedronate concentration versus absorbance. The intercept (*A*), slope (*B*) and coefficient of correlation (*r*) were evaluated for five independent concentration by duplicated (*n* = 10). The linearity was studied over the range 4.3 and 87.1 μ g/mL (range linear of concentration, RLC). Student's *t*-test was applied to results.

Precision was determined by subjecting the same standard solution containing 17 μ g/mL RI to HPLC analysis six times within a week. Results were expressed as % RSD (relative standard deviation).

The accuracy of the method is determined by the calculating the recoveries for nine RI solutions (*n* = 9) at three different concentrations (15, 30 and 45 μ g/mL) and expressed as percentage of recovery, %R(*n*).

Limit of detection (LOD) and limit of quantitation (LOQ) were calculated using the following expressions [21]:

$$LOD = \frac{3,3 \sigma}{B} \quad (1)$$

$$LOQ = \frac{10 \sigma}{B} \quad (2)$$

where σ is the standard deviation (SD) of the response and *B* is the slope of the calibration curve. Three RI solutions in phosphate buffer corresponding to concentrations in the range 2–10 μ g/mL were used, which were performed in triplicate with two injections per point and the standard deviation (SD) of *y* intercepts of regression lines was used as σ in Eqs. (1) and (2).

2.10. In vitro release of risedronate from membranes

Drug release experiments with membranes (4.7 cm diameter) including different amount of RI were carried out were performed using the dissolution test of transdermal delivery systems using a dissolution apparatus (TDT-08L, Electrolab) containing 0.1 M Phosphate buffer (PBS, pH = 7.4) at 37 °C with a paddle stirring rate of 50 rpm [22]. At appropriate times (every 2 min during the initial 10 min, then every 5 min until 30 min, every 10 min until 1 h, every hour until 5 h, and finally every day for 9 days), the supernatants were removed and replaced by 2.0 mL of fresh buffer. The time-dependent release of the drug was followed by monitoring the amount of RI present in the supernatant medium through RP-HPLC methodology, before described.

The temporal dependence of the RI released at time *t*, from the membrane of thickness 2 L was analyzed to identify release kinetics arising from multiple release phenomena, and by evaluating the release exponent (*n*) over time periods corresponding to <60% drug loss [23, 24]. *L* is the half thickness of the polymeric membrane, as was defined in the mathematical model. Drug delivery is considered to be governed by Fickian diffusion when *n* = 0.5 whereas relaxation behavior (zero-order release) is suggested when *n* = 1. Values of *n* between 0.5 and 1.0 indicate anomalous (non-Fickian) kinetics.

3. Results and discussion

3.1. Drug/copolymer interaction study

The study of the existence of interactions between the matrix and the RI was performed by comparing the spectra of copolymer, poly(VA-co-DOF), and the matrix containing risedronate (6% (w/w)), which are shown in Fig. 2.

No significant displacement of the FTIR bands of the copolymer including RI was observed in comparison to the band corresponding to pure copolymer which suggests that, at the tested concentration, there are not obvious interactions between both components.

The glass transition temperature (*T_g*) was determined by differential scanning calorimetry. Fig. 3 show the DSC analysis of poly(VA-co-DOF) and copolymer including 6% (w/w) RI.

It is observed a decrease of *T_g* from 16.2 °C for the copolymer to –2.6 °C for the sample including the bisphosphonate. It is known that the formation of specific interactions drug-polymer leads to an increase of *T_g* above the theoretical value, whereas if the drug-polymer interaction is less than the drug-drug and polymer-polymer interactions, the *T_g* value obtained will be lower than expected value [25]. The decrease in the glass transition temperature of the material can be understood if one considers that the addition of the drug causes a plasticizing effect on the polymer, generating an increase of free volume and favoring the catenary movement [26]. These results are consistent with the FTIR analysis of the mixture; no significant interaction between the copolymer and the bisphosphonate is noticed, and if there is any, it is negligible in relation to the interactions of the components among themselves.

3.2. Membrane characterization

The membranes prepared including 6% (w/w) and 12% (w/w) RI, with thickness of 280 \pm 62 μ m and 277 \pm 65 μ m, respectively, had good flexibility and transparency, smooth and uniform surface, as can be seen in Fig. 4(a and b).

Membranes were also observed by optical microscopy (illuminated below), as can be seen in Fig. 4(c, d), in which is observed the RI dispersion in the matrix as dark areas dispersed included in a transparent matrix, presented as clear zones. Both films exhibit a highly homogeneous distribution of the drug.

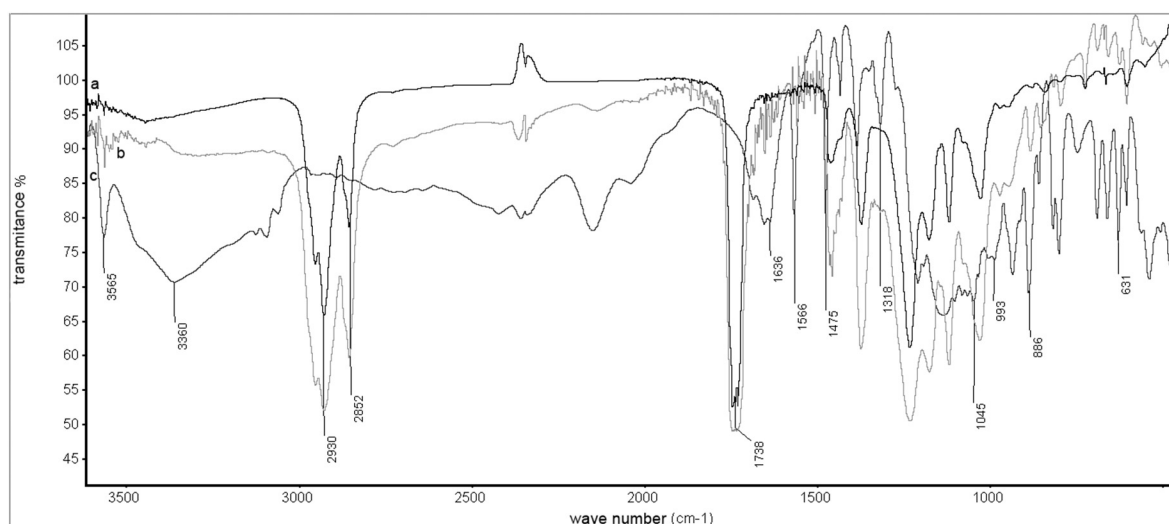


Fig. 2. FTIR of poly(VA-co-DOF) (a), copolymer including 6% (w/w) (b) and risedronate (c).

3.3. Drug load efficiency and stability solutions

Charging efficiency of the active ingredient included in delivery systems is an essential data to perform a correct study release profiles. The percentages RI mass deposited in the membranes were evaluated using the indirect method previously described and expressed as percentage in Table 1. The results show high efficiency of bisphosphonate load.

Stability testing of drugs is required to ensure the integrity of pharmaceutical product and their properties both during their valuation as during its useful life. In this work, the stability determination of the solutions of RI was carried out in phosphate buffer at 34 °C for 9 days, finding that there was no significant decrease in the title of the two standard solutions evaluated ($15.8 \pm 0.7 \mu\text{g/mL}$; $53.6 \pm 0.4 \mu\text{g/mL}$), nor the presence of other populations was observed in the chromatographic profile. Additionally, the UV-Vis spectrum of each solution on different days was analyzed, in order to determine the existence of bands shift or appearances of new bands, resulting from possible drug degradation in function of the time. Fig. 5 shows that no significant change is observed in the spectrum, demonstrating that RI solutions were stable under the conditions studied over the time period assessed.

3.4. HPLC analysis of risedronate

The selection of ion-pair reverse-phase high-performance liquid chromatography (RP-HPLC) method for the quantification of RI was based on the known of its high sensibility, ruggedness and accuracy, making it a useful tool not only for assay purposes, but impurities or degradation products analysis as well. The developed method used phosphate buffer and methanol mixture (75:25 (v/v)) as mobile phase which includes tetrabutylammonium bromide as ion-pair agent. The purpose of this reagent is to produce an association with the analyte in order to reduce its retention in the chromatographic column, which could result in a tailing effect. Fig. 6 shows the chromatographic profile of a RI sample, for which the elution time was $7.78 \pm 0.03 \text{ min}$ ($n = 8$).

The validation of the chromatographic method was determined through the parameters presented in the Table 2.

It may be noted that the value for the parameter % RSD = 0.4, suggests that the method has sufficient precision (acceptance criteria: RSD < 2%) [27].

The linearity of the method between the peak area and the concentration of risedronate was studied over the range (RLC) 4.3 $\mu\text{g/mL}$ and

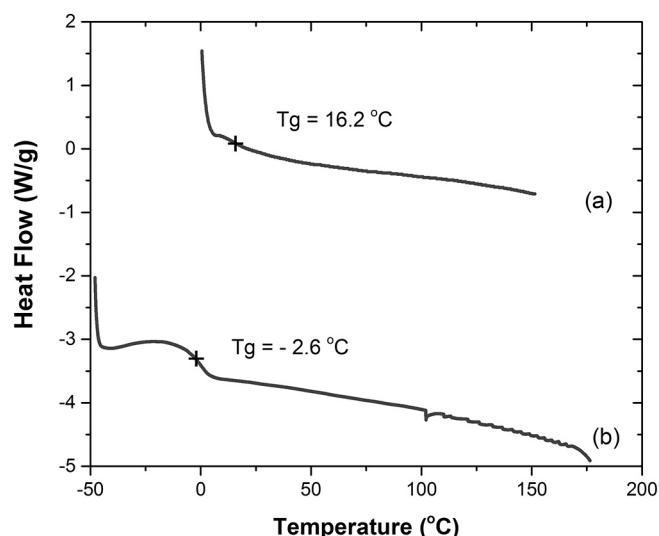


Fig. 3. DSC thermogram of poly(VA-co-DOF) without (a) and with 6% (w/w) RI (b).

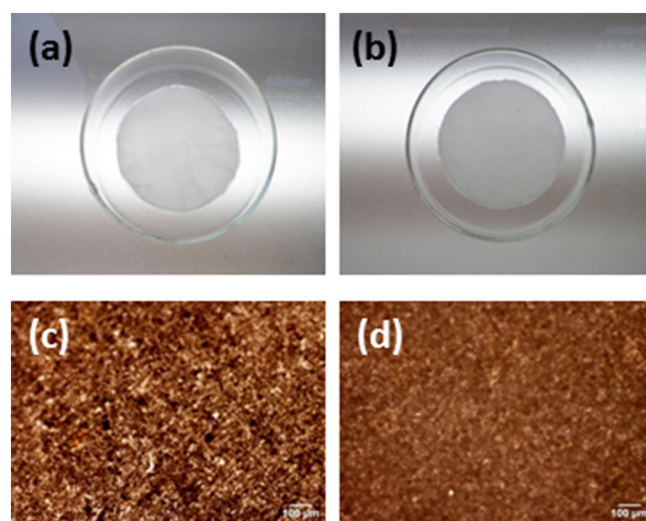


Fig. 4. Photograph (a, b) and light micrographs (c, d) of copolymer membrane including 6% (w/w) RI (a, c) and 12% (w/w) RI (b, d). (For interpretation of the references to color in this figure legend, the reader is referred to the web version of this article.)

Table 1
Percentage of loading efficiency.

| System | Drug loading (mean ± SD) (%) <i>n</i> = 3 | Drug loading efficiency (mean ± SD) (%) <i>n</i> = 3 |
|--------------------|---|--|
| Copolymer + 6% RI | 5.97 ± 0.01 | 99.60 ± 0,001% |
| Copolymer + 12% RI | 11.8 ± 0.3 | 99,8 ± 0,1% |

SD = standard deviation.

87.1 µg/mL. Starting from the calibration curve, the slope (A), intercept (B), the standard deviation values of the slope (S_A) and intercept (S_B) along with the correlation coefficient (r^2) were evaluated and are presented in Table 2. A Student's *t*-test was performed to determine whether the experimental intercepts (A) of the regression equations were significantly different from the theoretical zero value. The test is based on the calculation of the quantities $t = A/S_A$, and their comparison with tabulated data of the *t*-distribution. As it is presented in Table 2 the calculated *t*-values (3.05) do not exceed the 95% criterion of $t_p = 3.18$ for $f = n - 2 = 3$ degrees of freedom, which denotes that the intercept of regression line is not significantly different from zero. The linearity was also confirmed through the Olkin-Pratt test, which gave a $G(r) = 0.9998$ value, which indicated that the regression showed a good linearity [28].

The accuracy of the method was evaluated by means of recovery tests at three concentration levels (15, 30 and 45 µg/mL), triplicate measurements ($n = 9$), and expressed as percentage recoveries %R(*n*). The statistical analysis (Student's *t*-test) demonstrated that the method is suitable for evaluation of the accurately weighted amount of drug and therefore it has sufficient accuracy for use.

The limits of detection (LOD) and quantification (LOQ) were found to be 0.38 µg/mL and 1.17 µg/mL, respectively; these values were similar to those reported by other authors [29]. The statistical evaluation of the developed RP-HPLC method presented good linearity, reproducibility and accuracy, indicating that it can be used for the simple and reliable determination of RI.

3.5. Risedronate release kinetic analysis

Fig. 7(a) and (b) shows the release profiles of risedronate from the membrane containing two drug concentrations (6 and 12% (w/w)) until a maximum time of 216 h.

In the case of the membrane with the lowest drug content (6% (w/w)) the observed release curves showed a rapid initial burst

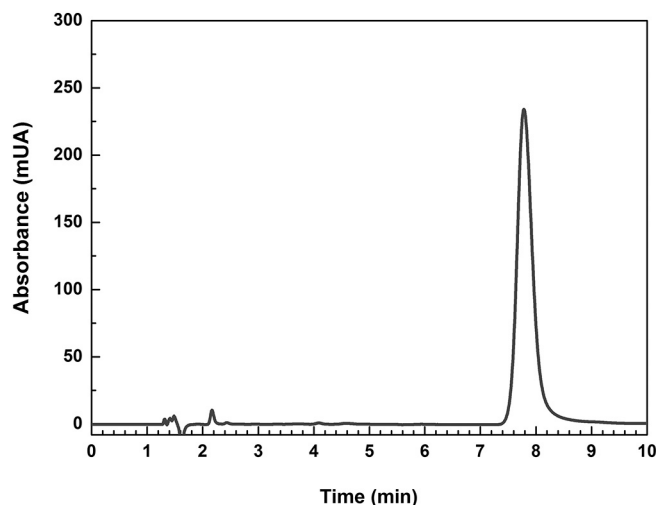


Fig. 6. Representative RP-HPLC chromatograms of risedronate solution.

release reaching the plateau around the first hour followed by a very slow drug release. This behavior could be due to rapid diffusion of drug on the surface of membrane, with another portion retained in deeper core of the matrix. In the case of the membrane including 12% (w/w) of RI, the percentage of the burst released portion of the drug is considerably lower with the following slower release segment approaching to the plateau between the 74 and 96 h. It is also remarkable that in both cases the final released percentage of risedronate was close to 70%, while 30% is retained in the polymer matrix.

In order to determine and understand the mechanism of release of RI from the TDDS designed in this study, the percentage of drug release data were fitted to Ritger-Peppas mathematical release model [30]. The following equation was used:

$$\frac{M_t}{M_\infty} = kt^n \quad (3)$$

where M_t/M_∞ is the fraction of drug release at time *t*, M_t is the amount of drug released at time *t*, M_∞ is the total amount of drug released at ∞ time (plateau), *k* is the kinetic constant and *n* is the diffusion exponent. This last parameter was estimated from the linear regression of $\log(M_t/M_\infty)$ versus $\log t$ at short time (<60% drug release) as can be seen in the insert of Fig. 7(a and b). The model of Ritger-Peppas proposes that when $n = 0.5$ the release behavior followed a Fickian diffusion mechanism, while $0.5 < n < 1$, indicates anomalous or non-Fickian diffusion which denotes a combinations of diffusion and erosion controlled rate release. When $n = 1$, it indicates case II, while $n > 1$ suggest super case transport II [31]. In our system the *n* values were 1.37 and 1.05 for 6% (w/w) and 12% (w/w) of RI, respectively; which correspond to super case transport II. These results suggest that the drug release is the consequence of a plasticizing process in the gel layer produced by the increased mobility of polymer chains resulting from a decrease in the attractive forces between them.

Table 2
Analytical figures of merit of chromatographic method.

| Parameter | Result |
|---------------------|----------------|
| %RSD | 0,4 |
| RLC (µg/mL) | 4.36–87.14 |
| $A \pm S_A$ | –78.70 ± 25.82 |
| $B \pm S_B$ | 55.16 ± 0.48 |
| r^2 | 0.9994 |
| A/S_A | 3.05 |
| LOD (µg/mL) | 0.38 |
| LOQ (µg/mL) | 1.17 |
| %R(<i>n</i>) ± Sd | 98.0(9) ± 3.4 |

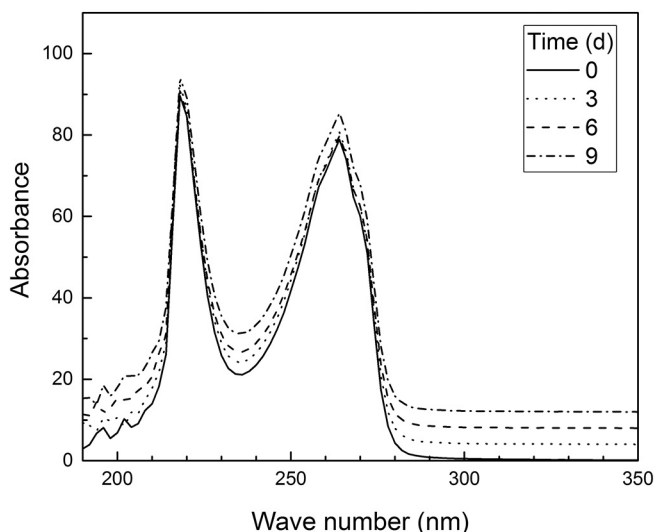


Fig. 5. UV-Vis spectrum of RI solution at 34 °C, at different times, during 9 days.

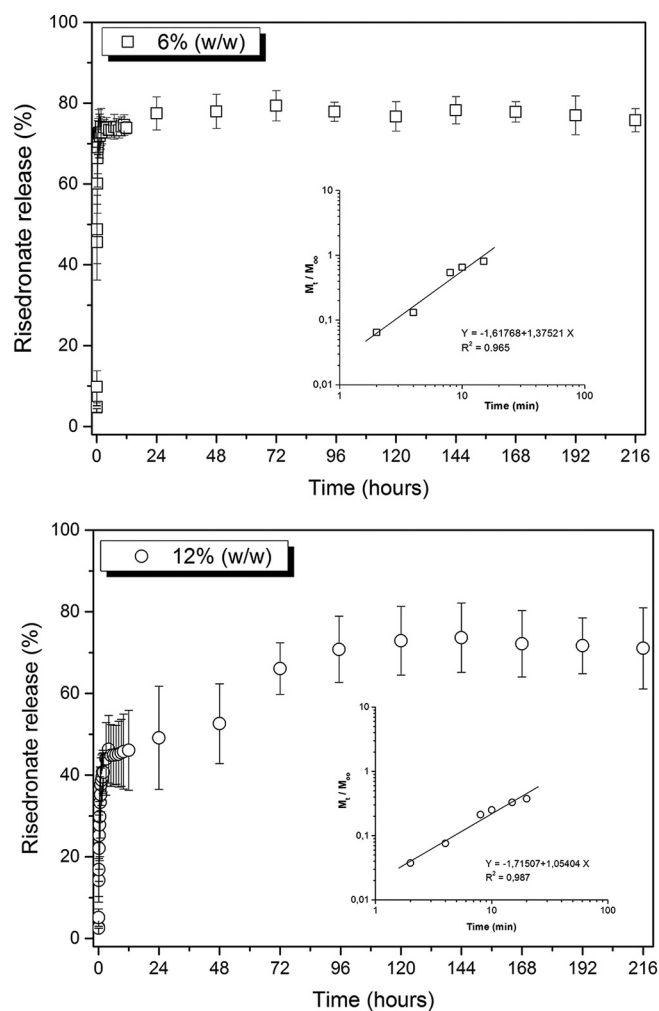


Fig. 7. Release profiles of risedronate from membrane with different drug content: 6% (w/w) (a) and 12% (w/w) (b). Inset: log-log graph of the kinetic analysis at the initial times.

This complex transport mechanism has also been observed in literature in other transdermal delivery systems [32,33].

4. Conclusions

A novel TDDS of risedronate was designed based on a fumaric copolymer, poly(VA-co-DOF), previously synthesized. Neither significant interaction drug/copolymer was observed, as demonstrated by FTIR spectra and calorimetric analysis; risedronate only cause a plasticizing effect on the macromolecular structure. Membrane including 6% and 12% (w/w) of RI exhibited good flexibility, transparency and high homogeneity of drug distribution. The methodology used for the drug incorporation into membrane proved to be highly efficient, and the stability test, through HPLC and UV spectroscopy assay, demonstrated that the RI solutions were stable up to time of evaluation (9 days). RP-HPLC methodology development for RI evaluation was validated and showed that it is suitable for the quantitative determination of the drug. The drug release profiles show that 70% of the drug is released after 1 h when the initially charged drug was 6% (w/w). On the other hand, the same percentage of drug released (70%) was observed after 96 h in the case of an initial charge of 12% (w/w) of RI. The release kinetics analysis through Ritger-Peppas model indicated that the system exhibited a behavior which could be fitted within super case transport II, which suggest a complex transport mechanism, regulated by the mobility of the polymer chains. Altogether, these results demonstrated that the RI

TDDS developed could be a potentially useful alternative for the treatment of osteoporosis.

Acknowledgments

This work was financially supported by grants from Facultad de Ciencias Exactas, Universidad Nacional de La Plata (UNLP, 11/X644). Magalí Pasqualone is indebted to CONICET for the fellowship awarded.

References

- [1] C. Ramachandran, D. Fleisher, Transdermal delivery of drugs for the treatment of bone diseases, *Adv. Drug Deliv. Rev.* 42 (2000) 197–223.
- [2] S.H. Tella, J.C. Gallagher, Prevention and treatment of postmenopausal osteoporosis, *J. Steroid Biochem. Mol. Biol.* 142 (2014) 155–170.
- [3] R.A. Lobo, J.H. Pickar, J.C. Stevenson, W.J. Mack, H.N. Hodis, Back to the future: hormone replacement therapy as part of a prevention strategy for women at the onset of menopause, *Atherosclerosis* (2016 Oct 6) pii: S0021-9150(16)31408-3 <http://dx.doi.org/10.1016/j.atherosclerosis.2016.10.005>.
- [4] Y. Zhang, L. Wei, R.J. Miron, B. Shi, Z. Bian, Bone scaffolds loaded with siRNA-Semaphorin4d for the treatment of osteoporosis related bone defects, *Sci. Rep.* 6 (2016) 26925.
- [5] M. Fazil, S. Baboota, J.K. Sahni, J. Ali Ameenudazzafar, Bisphosphonates: therapeutics potential and recent advances in drug delivery, *Drug Deliv.* 1 (2015) 1–9.
- [6] R. Schenk, D.P. Eggi, D.P. Fleisch, S. Rosini, Quantitative morphometric evaluation of the inhibitory activity of new aminobisphosphonates on bone resorption in the rat, *Calcif. Tissue Int.* 38 (1986) 342–349.
- [7] M.R. Watts, A.H. Ellims, D.S. Eccleston, Acute myopericarditis following intravenous zoledronic acid for the treatment of Paget's disease, *Med. J. Aust.* 200 (2014) 150.
- [8] E.A. Sigua-Rodriguez, R. da Costa Ribeiro, A.C. de Brito, N. Alvarez-Pinzo, J.R. de Albergaria-Barbosa, Bisphosphonate-related osteonecrosis of the jaw: a review of the literature, *Int. J. Dent.* 2014 (2014) 192320.
- [9] L.R. Garzoni, M.C. Waghbi, M.M. Baptista, S.L. de Castro, M.N. Meirelles, C.C. Britto, R. Docampo, E. Oldfield, J.A. Urbina, Antiparasitic activity of risedronate in a murine model of acute Chagas' disease, *Int. J. Antimicrob. Agents* 23 (2004) 286–290.
- [10] P.D. Papapetrou, Bisphosphonate-associated adverse events, *Hormones (Athens)* 8 (2009) 96–110.
- [11] H. Hirabayashi, T. Sawamoto, J. Fujisaki, Y. Tokunaga, S. Kimura, T. Hata, Dose-dependent pharmacokinetics and disposition of bisphosphonic prodrug of diclofenac based on osteotropic drug delivery system (ODDS), *Biopharm. Drug Dispos.* 23 (2002) 307–315.
- [12] D.F. Stamatialis, B.J. Papenburg, M. Gironés, S. Saiful, S.N.M. Bettahalli, S. Schmitmeier, M. Wessling, Medical applications of membranes: drug delivery, artificial organs and tissue engineering, *J. Membr. Sci.* 308 (2008) 1–34.
- [13] A. Choi, H. Ganga, I. Chun, H. Gwak, The effects of fatty acids in propylene glycol on the percutaneous absorption of alendronate across the excised hairless mouse skin, *Int. J. Pharm.* 357 (2008) 126–131.
- [14] K. Kusamori, H. Katsumi, M. Abe, A. Ueda, R. Sakai, R. Hayashi, Y. Hirai, Y.S. Quan, F. Kamiyama, T. Sakane, A. Yamamoto, Development of a novel transdermal patch of alendronate, a nitrogen-containing bisphosphonate, for the treatment of osteoporosis, *J. Bone Miner. Res.* 25 (2010) 2582–2591.
- [15] S.H. Nam, Y.J. Xu, H. Nam, G.W. Jin, Y. Jeong, S. An, J.S. Park, Ion pairs of risedronate for transdermal delivery and enhanced permeation rate on hairless mouse skin, *Int. J. Pharm.* 419 (2011) 114–120.
- [16] M. Pasqualone, T.G. Oberti, H.A. Andretta, M.S. Cortizo, Fumarate copolymers-based membranes overlooking future transdermal delivery devices: synthesis and properties, *J. Mater. Sci. Mater. Med.* 24 (2013) 1683–1692.
- [17] H. Fleisch, *Bisphosphonates in Bone Disease: From the Laboratory to the Patient*, 4th Ed., Academic Press, San Diego, 2000.
- [18] D.V.N. Srinivasa Rao, R. Dandala, R. Lenin, M. Sivakumaran, S. Shivashankar, A. Naidu, A facile one pot synthesis of bisphosphonic acids and their sodium salts from nitriles, *ARKIVOC xiv* (2007) 34–38.
- [19] V. Dissette, P. Bozzi, C.A. Bignozzi, A. Dalpiaz, L. Ferraro, S. Beggiato, E. Leod, E. Vighid, L. Pasti, Particulate adducts based on sodium risedronate and titanium dioxide for the bioavailability enhancement of oral administered bisphosphonates, *Eur. J. Pharm. Sci.* 41 (2010) 328–336.
- [20] P. Araujo, Key aspects of analytical method validation and linearity evaluation, *J. Chromatogr. B* 877 (2009) 2224–2234.
- [21] International Conference on Harmonization (ICH), *Validation of Analytical Procedures: Text and Methodology*, International Conference on Harmonization of Technical Requirements for the Registration of Pharmaceuticals for Human Use [Q2 (R1)], 2005.
- [22] M. Guyot, F. Fawaz, Design and in vitro evaluation of adhesive matrix for transdermal delivery of propranolol, *Int. J. Pharm.* 204 (2000) 171–182.
- [23] T. Higuchi, Mechanism of sustained-action medication: theoretical analysis of rate of release of solid drugs dispersed in solid matrices, *J. Pharm. Sci.* 52 (1963) 1145–1149.
- [24] N.A. Peppas, Analysis of Fickian and non-Fickian drug release from polymers, *Pharm. Acta Helv.* 60 (1985) 110–111.
- [25] Chap 2: crystalline and amorphous solids, in: G.G.Z. Zhang, D. Zhou, Y. Qiu, Y. Chen, G.G.Z. Zhang, L. Liu, W.R. Porter (Eds.), *Developing Solid Oral Dosage Forms: Pharmaceutical Theory and Practice*, 1ra ed., Academic Press, Amsterdam 2009, pp. 25–60.

- [26] Y. Li, H. Pang, Z. Guo, L. Lin, Y. Dong, G. Li, M. Lu, C. Wu, Interactions between drugs and polymers influencing hot melt extrusion, *J. Pharm. Pharmacol.* 66 (2013) 148–166.
- [27] A.P.P. Cione, M.J. Liberale, P.M. da Silva, Development and validation of an HPLC method for stability evaluation of nystatin, *Braz. J. Pharm. Sci.* 46 (2010) 305–310.
- [28] I. Olkin, J.W. Pratt, Unbiased estimation of certain correlation coefficients, *Ann. Math. Stat.* 29 (1958) 201–211.
- [29] M.C. Damle, L.B. Birajdar, Development and validation of stability-indicating hplc method for estimation of risedronate sodium, *World J. Pharm. Pharm. Sci.* 4 (2015) 644–653.
- [30] P.L. Ritger, N.A. Peppas, A simple equation for description of solute release. I. Fickian and non-Fickian release from non-swelling devices in the form of slabs, spheres, cylinders or discs, *J. Control. Release* 5 (1987) 23–36.
- [31] P. Costa, J.M.S. Lobo, Modelling and comparison of dissolution profiles, *Eur. J. Pharm. Sci.* 13 (2001) 123–133.
- [32] Y.S. Tanwar, C.S. Chauhan, A. Sharma, Development and evaluation of carvedilol transdermal patches, *Acta Pharm. (Zagreb, Croatia)* 57 (2007) 151–159.
- [33] S. Kumar Dey, P. Kumar De, T. Sen, V. Shankar, U. Banerjee, Formulation and in vitro evaluation of transdermal matrix patches of diclofenac sodium, *J. Pharm. Res.* 4 (2011) 3593–3596.